International Journal of Fracture 30 (1986) 79–102

Energy release rate along a three-dimensional crack front in a thermally stressed body

C.F. SHIH, B. MORAN and T. NAKAMURA

Division of Engineering, Brown University, Providence, RI 02912, USA

(Received 10 June 1985; in revised form 10 October 1985)

Abstract

Based on a line-integral expression for the energy release rate in terms of crack tip fields, which is valid for general material response, a (area/volume) domain integral expression for the energetic force in a thermally stressed body is derived. The general three-dimensional finite domain integral expression and the two-dimensional and axisymmetric specializations for the energy release rate are given. The domain expression is naturally compatible with the finite element formulation of the field equations. As such it is ideally suited for efficient and accurate calculation of the pointwise values of the energy release rate along a three-dimensional crack front. The finite element implementation of the domain integral corresponds to the virtual crack extension technique. Procedures for calculating the energy release rate using the numerically determined field solutions are discussed. For illustrative purposes several numerical examples are presented.

1. Introduction

Several structural integrity problems with the nuclear steam supply systems can be addressed by a nonlinear fracture mechanics methodology. A problem of some urgency is the integrity of pressurized water reactors during a severe overcooling transient. One important aspect of the integrity evaluation is the variation of the intensity of the stresses and deformation during the transient in the vicinity of the surface cracks located in the weldments in the beltline region. Recent progress in a phenomenological approach to the initiation of crack growth and the subsequent quasi-static crack growth and loss of stability under monotonic load histories has been reviewed in [1]. Within the framework of the approach and under conditions referred to as J-dominance, the value of the J-integral is a measure of the intensity of the crack tip fields and can be used to correlate the initiation of crack growth in plastically deforming solids.

Under J-dominant conditions, the intensity of the stress and deformations within the vicinity of the three-dimensional crack front is given by the pointwise value of J [1,2]. However a determination of the pointwise J values along a crack front during a transient thermo-mechanical loading is not an easy task. In three-dimensional cracked bodies, the plane strain two-dimensional fields are only asymptotically approached at the crack front, so that the two-dimensional line integral definition of J may be used only very near to the crack tip. It is precisely for points arbitrarily close to the crack tip for which accurate finite element calculation of field quantities is most difficult. To circumvent this difficulty finite (area/volume) domain integrals have been introduced for the computation of the energy release rate.

It is now generally accepted that accurate pointwise values of the energy release rate $J(s)$ along a three-dimensional crack front can be obtained by the virtual crack extension

(VCE) technique [3–7,25,26]. While it is known that thermal strains, body force and crack face traction can be readily included in the VCE technique we are unaware of a direct derivation. Such a derivation follows directly from a fundamental expression for the crack tip energy flux integral which underlies virtually all crack tip integrals in use in fracture mechanics [8–11] and which has been generalized to include thermal strains (e.g. Nguyen [12]). In the next section we give a concise derivation of the domain integral expression for the energy release rate in a thermo-mechanical field using the crack tip energy integral as the starting point. In fact some existing expressions which are similar to those we present in this paper were obtained by imprecise applications of energy balance. The finite element implementation of the domain integral formulation which corresponds to the VCE technique is outlined in Section 3. In Appendix A we show how J may be interpreted as an amplitude parameter for the crack tip singular fields of the thermal stress problem. An alternative derivation of the pointwise energy release rate expression is given in Appendix B for the case of a mathematically sharp crack and it is shown how the axisymmetric and two-dimensional specializations follow readily from the three-dimensional result.

2. A domain integral expression for the energy release rate

2.1. Two-dimensional specialization

For the moment we consider a two-dimensional body and direct our attention to a line crack along the x_1 axis. For arbitrary crack tip motion (but restricted to crack advance along the x_1 axis) under dynamic conditions the energy release per unit crack advance is

$$J = \lim_{\Gamma \to 0} \int_{\Gamma} \left((W+T)n_1 - \sigma_{ij} n_i \frac{\partial u_j}{\partial x_1} \right) \mathrm{d}C \tag{2.1}$$

where W and T are the stress work and kinetic energy densities respectively, σ_{ij} and u_i are the Cartesian components of the stress and displacement, n_i is the unit vector normal to Γ and $\mathrm{d}C$ is the arc length as depicted in Fig. 1. In the context of linear elastic material response, the result (2.1) was proposed by Atkinson and Eshelby [8] and independently derived by Kostrov and Nikitin [9] and Freund [10]. It has since been recognized that (2.1) is also valid for nonelastic material response. As noted by Nakamura et al. [11], "the general result (2.1) underlies virtually all crack tip energy integrals that have been defined and applied in fracture mechanics in the sense that each may be derived from (2.1) by invoking the appropriate restrictions on material response (through W) and on crack tip motion." Several illustrations and applications are also given in [11]. While result (2.1)

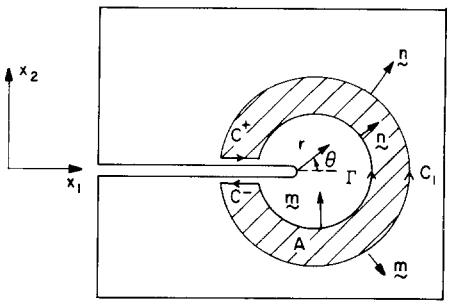

Figure 1. Closed contour $C = C_1 - \Gamma + C^+ + C^-$ encloses a simply connected region A; note that $\boldsymbol{m} = -\boldsymbol{n}$ on Γ. In the presence of thermal strain, body force and/or crack face traction domain A must include the crack-tip region ($r \to 0^+$).

was obtained from purely mechanical considerations, a more general result can be derived from a thermodynamic approach (see Nguyen [12]). With the usual reinterpretation of the field quantities with reference to the undeformed configuration, (2.1) also holds in the context of finite deformation.

Under quasi-static condition, $T = 0$, and (2.1) reduces to

$$J = \lim_{\Gamma \to 0} \int_{\Gamma} \left(W\delta_{1i} - \sigma_{ij} u_{j,1} \right) n_i \, \mathrm{d}C \tag{2.2}$$

For a deformation theory solid, and in the absence of body force, thermal strains and crack face tractions, the integral in (2.2) is path-independent and its value does not depend on a limiting process in which the crack tip contour Γ is shrunk onto the crack tip. The above result is due to Rice [13]. For this important case, the contour integral value for J (2.2) can be accurately and readily extracted from the finite element fields remote from the crack tip. We note that Eshelby introduced the conservation integral (2.2) in the context of the force on a dislocation or point defect; under isothermal conditions the bracketed quantity is the x_1 component of the energy-momentum tensor (see [14] and [15]).

Directing our attention to a deformation theory solid, we follow Li et al. [7] and rewrite (2.2) in the form

$$J = \int_C \left[\sigma_{ij} u_{j1} - W\delta_{1i} \right] m_i q_1 \, \mathrm{d}C - \int_{C^+ + C^-} \sigma_{2j} u_{j,1} m_2 q_1 \, \mathrm{d}C. \tag{2.3}$$

Here the closed curve $C = C_1 + C^+ + C^- - \Gamma$, q_1 is a sufficiently smooth function in the region enclosed by C that is unity on Γ and vanishes on C_1 and m_j is the outward normal as depicted in Fig. 1; note that $m_1 = 0$, $m_2 = \pm 1$ on the crack faces, and $m_j = -n_j$ on Γ. The last term in (2.3) vanishes for traction free crack faces.

Within the framework of an uncoupled quasi-static thermoelastic (deformation plasticity) theory, the strain is written as the sum of an elastic part ϵ_{ij}^e, a volume preserving (deviatoric) plastic part e_{ij}^p and a thermal part

$$\epsilon_{ij} = \epsilon_{ij}^e + e_{ij}^p + \alpha\theta\delta_{ij} \tag{2.4}$$

where α is the coefficient of thermal expansion and the temperature θ (relative to the ambient temperature) is obtained from a (separate) heat conduction analysis. The elastic and plastic strains are given by

$$\epsilon_{ij}^e = \frac{1+\nu}{E} s_{ij} + \frac{1-2\nu}{3E} \sigma_{kk}\delta_{ij}, \quad e_{ij}^p = \frac{3}{2}\left(\frac{1}{E_s} - \frac{1}{E} \right) s_{ij} \tag{2.5}$$

and the inverted relations are

$$s_{ij} = \left(\frac{E_s}{1+\nu_s} \right) e_{ij}, \quad \sigma_{kk} = \left(\frac{E}{1-2\nu} \right) (\epsilon_{kk} - 3\alpha\theta), \quad \nu_s = \frac{1}{2} + \frac{E_s}{E}\left(\nu - \tfrac{1}{2} \right). \tag{2.6}$$

Here s_{ij} and e_{ij} are the deviatoric stresses and strains, E is Young's modulus, ν is Poisson's ratio, E_s is the secant modulus and ν_s is the effective Poisson's ratio. We make the additional assumption that thermal strains are bounded With this restriction, a definition of W which can be used in (2.1), (2.2) and therefore in (2.3) as well is

$$W(\epsilon_{ij};\, \theta) = \int_0^{\epsilon_{ij}^m} \sigma_{ij} \, \mathrm{d}\epsilon_{ij}^m = \int_0^{e_{ij}} s_{ij} \, \mathrm{d}e_{ij} + \tfrac{1}{3} \int_0^{\epsilon_{ii}^e} \sigma_{kk} \, \mathrm{d}\epsilon_{ii}^e \tag{2.7}$$

i.e., W is a mechanical strain energy density where $\epsilon_{ij}^m = \epsilon_{ij} - \alpha\theta\delta_{ij}$ are the mechanical strains. For isothermal response, W may be identified with the free energy.

Applying the divergence theorem to the closed contour integral in (2.3), we get

$$J = \int_A \left[(\sigma_{ij} u_{j,1} - W\delta_{1i}) q_1 \right]_{,i} \, \mathrm{d}A - \int_{C^+ + C^-} \sigma_{2j} u_{j,1} m_2 q_1 \, \mathrm{d}C \tag{2.8}$$

where A is the simply connected (area) domain enclosed by C. We emphasize that the domain A includes the crack-tip region ($r \to 0^+$). Now invoke equilibrium and a standard result (we assume that W does not depend explicitly on x_i)

$$\sigma_{ij,j} + f_i = 0, \quad W_{,1} = q_{ij} \epsilon_{ij,1} - \alpha \sigma_{kk} \theta_{,1} \tag{2.9}$$

to obtain the desired domain expression for the energy release rate

$$J = \int_A \left\{ \left[\sigma_{ij} u_{j,1} - W\delta_{1i} \right] q_{1,i} + \left[\alpha \sigma_{ii} \theta_{,1} - f_i u_{i,1} \right] q_1 \right\} \, \mathrm{d}A - \int_{C^+ + C^-} t_i u_{i,1} q_1 \, \mathrm{d}C. \tag{2.10}$$

Here f_i is the body force per unit volume and t_i is the traction on the crack faces. If inertia cannot be neglected and W depends explicitly on x_i, the additional terms $\rho \, \partial^2 u_i / \partial t^2$ and $(\partial W / \partial x_1)_{\text{explicit}}$ must be included with the "body force" type terms which are weighted by q_1 in (2.10). ★

In the absence of thermal strain, body force and crack face traction, (2.10) reduces to

$$J = \int_A \left[\sigma_{ij} u_{j,1} - W\delta_{1i} \right] q_{1,i} \, \mathrm{d}A \tag{2.11}$$

which is the energy release rate expression given in [6,7]. Consistent with the path-independence of J [13], (2.11) is domain-independent in the sense that any annular (area) domain can be chosen for the purpose of evaluating J. In this case the choice of domain is often dictated by convenience and mesh design. With the presence of thermal strain, body force, and/or crack face traction, the domain of integration for (2.10) must include the near-tip region ($r \to 0^+$).

The function q_1 can be interpreted as imposing on the material points on Γ a unit translation in the x_1 direction while requiring the material points on C_1 to remain fixed. The material points within A are displaced according to any smooth interpolating function. Thus the (area) domain method of evaluating J can be interpreted as a virtual crack extension technique. In the context of a finite element model, Γ is the arc formed by the crack tip node/nodes. By letting C_1 coincide with the boundaries of different rings of elements surrounding the crack tip, J can be evaluated on alternate domains. A detailed discussion of these aspects is given in [3–7].

Similar expressions for the energy release rate containing two integrals, the integral in (2.2) taken along a remote contour and a domain integral for the thermal contributions, have been given by Wilson and Yu [16] and Aoki et al. [17]. Nevertheless there are important differences. In the absence of crack face traction, (2.10) is strictly a domain integral and the evaluation of the integral involves the same integration procedures used to obtain the stiffness matrix in the finite element method. Similarly the crack face traction contribution in (2.10) can be handled by the usual integration procedures for boundary forces/pressures. In other words the evaluation of (2.10) is a natural extension of the finite element solution process. Furthermore the present formulation can be directly generalized to obtain the energy release rate expression along a three-dimensional crack front. The result (2.10) is derived from the three-dimensional result for a sharp crack configuration in Appendix B.

★ With the inclusion of inertia terms in (2.10), J must be interpreted as the virtual energy release rate, i.e., J computed from (2.10) is the energy increment that would be released if the mechanical fields were frozen at the instant and the crack tip were given an increment of extension in the x_1-direction [11].

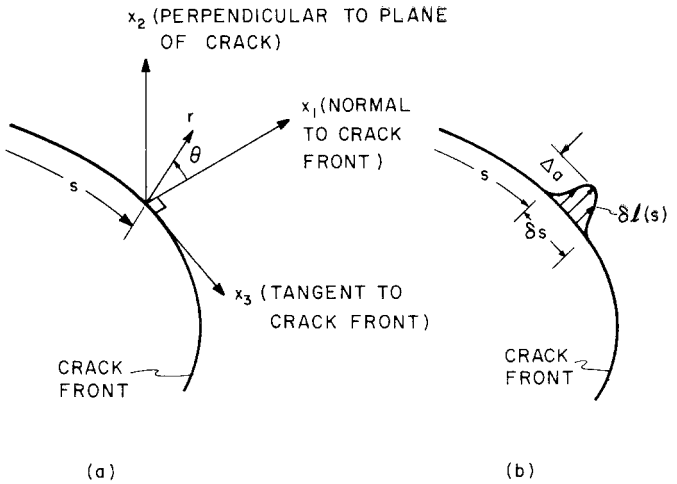

Figure 2. (a) Definition of local orthogonal Cartesian coordinates at the point s on the crack front; the crack plane is in the $x_1 - x_3$ plane.
(b) The function $\delta l(s)$ can be pictured as a virtual crack advance in the direction normal to the crack front in the crack plane.

2.2. Three-dimensional formulation

We consider a three-dimensional crack front with a continuously turning tangent. Imagine that the plane shown in Fig. 1 is now the $x_1 - x_2$ plane of the local orthogonal Cartesian system depicted in Fig. 2a. Asymptotically, as $r \to 0^+$, plane strain conditions prevail so that the three-dimensional fields approach the (plane strain) two-dimensional fields at the crack front. Thus (2.2) defines the pointwise energy release rate which we denote by $J(s)$. To develop a finite (volume) domain expression which will allow the determination of $J(s)$ along the crack front we now follow the procedure taken in [3–7].

Let $\delta l(s)$ denote the local crack front advance at the point s in the direction normal to the crack front and in the plane of the crack, and let $\mathrm{d}s$ denote the elemental arc length along the crack front as depicted in Fig. 2b. Then to within first order terms in δl

$$-\delta\pi = \bar{J}\Delta a = \int_{L_c} J(s)\delta l(s)\,\mathrm{d}s \tag{2.12}$$

where L_c denotes the line segment of crack front under consideration and δl is an arbitrary crack front advance. Here $-\delta\pi$ is the decrease in potential energy and $\bar{J}$ is therefore the energy released per unit of the finite segment of crack advance. By separately advancing various segments of the crack front, the arc-weighted pointwise $J(s)$ can be computed along a three-dimensional crack front.

To fix ideas and minimize nonessential manipulations we focus our attention on a notch with notch thickness h as shown in Fig. 3 and argue (heuristically) that $h \to 0$ is the sharp crack configuration of interest. The surface of the notch consists of faces S_A and S_B, with normals along x_2, and a face with a normal in the $x_1 - x_3$ plane. Now let the notch face S_t with normal m_k in the $x_1 - x_3$ plane advance $\Delta a\, l_k$ in the x_k direction, i.e.,

$$\Delta a\, l_k m_k = \delta l(s). \tag{2.13}$$

Furthermore restrict l_k to lie along S_t and to be a function of x_1 and x_3 only; thus $l_2 \equiv 0$. Using (2.2) and (2.13) in (2.12), we obtain

$$\bar{J}\Delta a = \Delta a \int_{S_t} \left[\sigma_{ij}u_{j,k} - W\delta_{ki}\right] l_k m_i\,\mathrm{d}S. \tag{2.14}$$

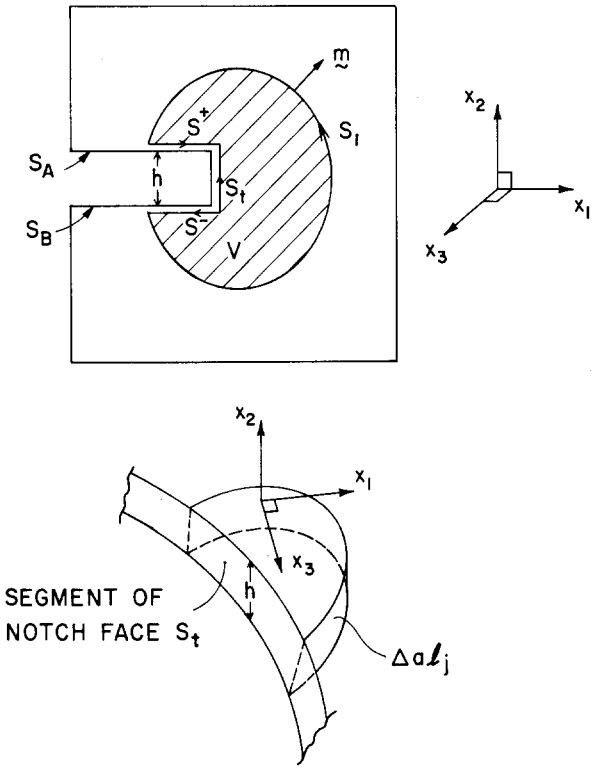

Figure 3. (a) Schematic of section of body and volume V in the $x_1 - x_2$ plane containing a notch of thickness h; note that $\boldsymbol{m} = -\boldsymbol{n}$ on S_t. (b) Schematic of notch face when the function $\Delta a l_j$ is interpreted as a virtual advance of a notch face segment in the direction normal to x_2.

As discussed in [7], when $\Delta a\, l_k$ corresponds to a translation, l_k can be taken outside of the integral sign and (2.14) gives $\bar{J} = l_k J_k$ where under isothermal conditions J_k are the translational conservation integrals (Budiansky and Rice [15]).

To develop a (volume) domain integral, we consider the simply connected volume, V, enclosed by the surfaces S_t, S^+, S^- and S_1 as depicted in Fig. 3. Furthermore introduce the functions q_k defined by

$$q_k = \begin{cases} l_k & \text{on } S_t \\ 0 & \text{on } S_1 \end{cases} \tag{2.15}$$

together with the requirement that q_k be sufficiently smooth in the volume V. Using (2.15), we can rewrite (2.14) in the form of an integral over the closed surface S ($S = S_1 + S^+ + S^- - S_t$) plus crack face terms,

$$\bar{J} = \int_S \left[\delta_{ij} u_{j,k} - W\delta_{ki}\right] m_i q_k \, \mathrm{d}S - \int_{S^+ + S^-} \sigma_{2j} u_{j,k} m_2 q_k \, \mathrm{d}S. \tag{2.16}$$

To arrive at (2.16) we have used these results $m_1 = 0$, $m_3 = 0$ ($m_2 = \pm 1$), on the crack faces; it may be noted that $l_2 = q_2 = 0$ everywhere.

We apply the divergence theorem to the closed surface integral in (2.16), and use (2.9) to get

$$\bar{J} = \int_V \left\{ \left[\sigma_{ij} u_{j,k} - W\delta_{ki}\right] q_{k,i} + \left[\alpha\sigma_{ii}\theta_{,k} - f_i u_{i,k}\right] q_k \right\} \mathrm{d}V - \int_{S^+ + S^-} t_i u_{i,k} q_k \, \mathrm{d}S. \tag{2.17}$$

We now let $h \to 0$ to obtain the desired expression for the energy decrease when a local

segment of the crack front advances by $\Delta a l_k$ in its plane. In the absence of body force, thermal strain and crack face traction, (2.17) is identical to the (volume) domain integral expression for J previously obtained [6,7].

The domain expression (2.17) gives the energy released by the body per unit of crack advance over a finite segment of the crack front. To a first approximation the pointwise energy release ratio is given by

$$J(s) = \frac{\bar{J}\Delta a}{\Delta a \int_{L_c} l_k(s) m_k(s)\, \mathrm{d}s} \tag{2.18}$$

where the term in the denominator is the increase of the crack area due to the virtual crack advance. A more precise procedure for calculating the pointwise energy release rate, which uses (2.17) and piecewise basis functions to represent $J(s)$ and $\delta l(s)$ along the crack front, is discussed in Section 3. The above results (2.17) and (2.18) are derived for the case of a sharp crack in Appendix B.

2.3. Axisymmetric specialization

We are now in a position to address the axisymmetric specialization of the 3-D formulation. To facilitate the derivation, we consider a narrow wedge of angular width $\mathrm{d}\phi$ (of a penny shaped crack in a solid of revolution) and separate the surface S_1 (introduced in Section 2.2) into three parts, the cylindrical surface S_c and the two end surfaces S_e^+ and S_e^- as shown in Fig. 4. We require q_1 be unity on S_t, vanish on S_c and vary smoothly in the volume V enclosed by S. Furthermore let q_1 depend only on the cylindrical coordinates r and z, stipulate that q_3 be given by $q_3 = -q_1\phi$ and set $q_2 = 0$

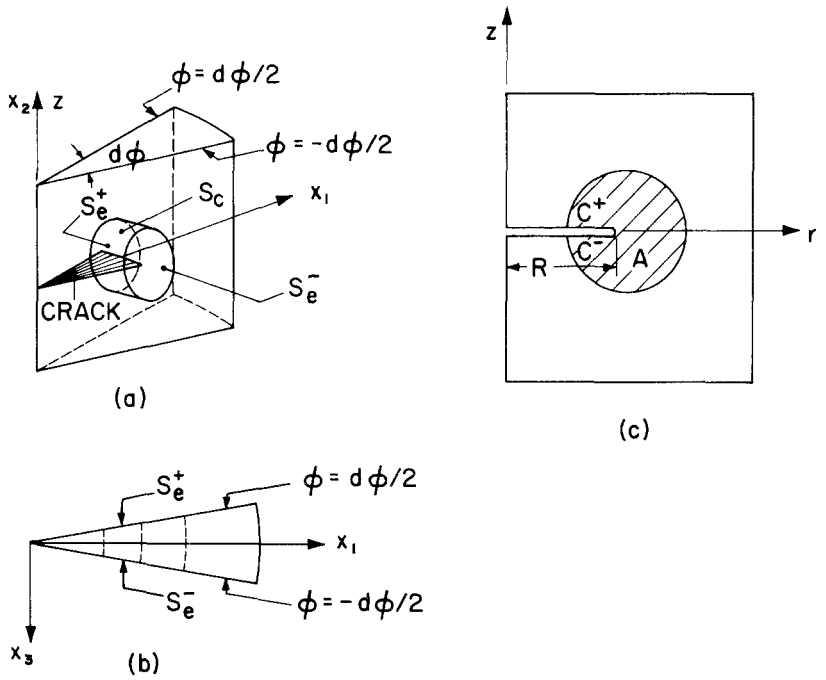

Figure 4. (a) A wedge of a solid of revolution containing an internal crack. The closed surface S consists of S_c, S_e^+, S_e^- (which are indicated), the crack faces S^+ and S^- and the crack front S_t. (b) Plan view of wedge. (c) The integration plane for the axisymmetric specialization; the domain A and the crack edges C^+ and C^- are indicated.

everywhere. As a consequence, q_k does not vanish on S_e^+ and S_e^- (note that q_k vanishes everywhere on S_1 in the general 3-D formulation). With q_k thus defined, the energy released by the body due to a unit advance of the crack front (of angular width $d\phi$) is

$$\bar{J} = \int_S \left[\sigma_{ij} u_{j,k} - W\delta_{ki}\right] m_i q_k \, dS - \int_{S^+ + S^-} \sigma_{2j} u_{jk} m_2 q_k \, dS$$

$$- \int_{S_e^+ + S_e^-} \left[\sigma_{ij} u_{j,k} - W\delta_{ki}\right] m_i q_k \, dS \qquad i, j, k = 1, 2, 3. \tag{2.19}$$

The latter equation which is appropriate for subsequent manipulations is a version of the general 3-D surface integral (2.16).

We take advantage of the axisymmetry to rewrite the fields in (2.19) and the domain of integration using cylindrical coordinates. It follows from the prescription of q_k that q_ϕ and q_z vanishe everywhere in V and that $q_3 = \pm q_r \, d\phi/2$ on S_e^+ and S_e^-. Applying the divergence theorem to the closed surface integral and noting that $m_\phi = \mp 1$ on S_e^+ and S_e^-, we get

$$\tilde{J} = \frac{\bar{J}}{d\phi} = \int_A \left\{ \left[\sigma_{\beta\gamma} u_{\gamma,r} - W\delta_{r\beta}\right] q_{,\beta} + \left[\alpha \, \mathrm{tr}(\sigma)\theta_{,r} - f_\gamma u_{\gamma,r}\right] q \right\} r \, dA$$

$$- \int_{C^+ + C^-} t_\gamma u_{\gamma,r} q r \, dC + \int_A \left[\sigma_{\phi\phi} \frac{u_r}{r} - W\right] q \, dA \tag{2.20}$$

where $\tilde{J}$ is the energy released per unit advance of crack front per unit (radian) angle. Here the domain of integration is the $r-z$ plane, the Greek indices β and γ range over the coordinates r and z, $\sigma_{\phi\phi}$ and u_r/r are the hoop stress and strain respectively, $q \equiv q_r$, $\mathrm{tr}(\sigma)$ denotes the trace of σ_{ij}, and $(\,)_{,r}$ denotes the partial derivative with respect to r. In the absence of thermal strain, a similar expression for J is given in [18].

By definition the energy release rate (per unit area of crack extension) is

$$J = \frac{\tilde{J}}{R} \tag{2.21}$$

where R is the radial distance from the z axis to the crack tip. A similar expression for the externally cracked body can be obtained in the same manner. In Appendix B we derive the result (2.20) in an alternative fashion as a specialization of the three-dimensional result for a sharp crack.

3. Finite element formulation for the domain integral method

The finite element formulation of the area/volume integral method for the energy release which we will henceforth refer to as the domain integral method has been discussed by Li et al. [7]. In that paper, the formulation of the area integral and the volume integral method is described in the context of the two-dimensional biquadratic (9-node) Lagrangian element and the three-dimensional triquadratic (27-node) Lagrangian element. For 2-D/3-D elastic-plastic crack analyses, there are some advantages for using the 9/27 node elements in the region surrounding the crack tip/front. By the appropriate placement of nodes and the collapsing of an element edge/surface into a point/line, the displacement gradients for the 9/27 node element contain terms of order $(1/\sqrt{r})$ or $(1/r)$ everywhere within the element [19,20,7]. These element fields are consistent with the continuum elastic and perfectly plastic near-tip fields for cracked bodies. A simple check will show that terms of order $(1/\sqrt{r})$ and $(1/r)$ are not always uniformly attained within the domain of similarly modified 20-node 3-D isoparametric elements. We also note that 9/27-node Lagrangian elements are better suited for elastic-plastic analysis where the (incompressible) plastic deformation dominates the overall structural behavior [21,22].

To demonstrate the computational versatility of (2.10) and (2.17), we outline their implementation in the context of the 4-node 2-D element and the 8-node 3-D element.

3.1. Two-dimensional and axisymmetric implementation

For isoparametric elements, the coordinates (x_1, x_2) in the physical space and the displacements (u_1, u_2) are written as

$$x_i = \sum_{K=1}^{4} N_K X_{iK}, \quad u_i = \sum_{K=1}^{4} N_K U_{iK}, \quad i = 1, 2 \tag{3.1}$$

where N_K are the bilinear shape functions, X_{iK} are the nodal coordinates and U_{iK} are the nodal displacements [23].

Consistent with the isoparametric formulation, we take q_1 within an element as

$$q_1 = \sum_{I=1}^{4} N_I Q_{1I} \tag{3.2}$$

where Q_{1I} are the nodal values for the I^{th} node. From the definition of q_1, if the I^{th} node is on Γ, $Q_{1I} = 1$, whereas if the I^{th} node is on C_1, $Q_{1I} = 0$. In the area between Γ and C_1, Q_{1I} will be taken to vary between 1 and 0. It may be noted that a particular choice of interpolation scheme for Q_{1I} is equivalent to selecting a particular weighting scheme for the field quantities between Γ and C_1. Using (3.1), (3.2) and the chain rule, the spatial gradient of q_1 within an element is given by

$$\frac{\partial q_1}{\partial x_j} = \sum_{I=1}^{4} \sum_{k=1}^{2} \frac{\partial N_I}{\partial \eta_k} \frac{\partial \eta_k}{\partial x_j} Q_{1I} \tag{3.3}$$

where $\partial \eta_k / \partial x_j$ is the inverse Jacobian matrix of the transformation (3.1).

With 2×2 Gaussian integration, the discretized form of the domain expression for the energy release rate (2.10) for plane strain and plane stress problems is

$$J = \sum_{\substack{\text{all} \\ \text{elements} \\ \text{in } A}} \sum_{p=1}^{4} \left\{ \left[\left(\sigma_{ij} \frac{\partial u_j}{\partial x_1} - W \delta_{1i} \right) \frac{\partial q_1}{\partial x_i} + \left(\alpha \sigma_{ii} \frac{\partial \theta}{\partial x_1} - f_i \frac{\partial u_i}{\partial x_1} \right) q_1 \right] \det\left(\frac{\partial x_k}{\partial \eta_k} \right) \right\}_p w_p$$

$$- \sum_{\substack{\text{all edges} \\ \text{on } C^+ + C^-}} \left\{ t_i \frac{\partial u_i}{\partial x_1} q_1 \right\} w. \tag{3.4}$$

Here the quantities within $\{\ \}_p$ are evaluated at the 4 Gauss points and w_p and w are the respective weights. The crack face traction contributions can be evaluated using the equivalent nodal forces and the spatial gradient of the nodal displacements or using the standard integration procedure for boundary pressures [23]. (Note that the integration is carried out only on element edges on C^+ and C^- with non-zero traction).

For the axisymmetric configuration, the discretized form of (2.20) is

$$\tilde{J} = \sum_{\substack{\text{all} \\ \text{elements} \\ \text{in } A}} \sum_{p=1}^{4} \left\{ \left[\left[\sigma_{\beta\gamma} u_{\gamma,r} - W \delta_{r\beta} \right] q_{,\beta} + \left[\alpha \operatorname{tr}(\sigma) \theta_{,r} - f_\gamma u_{\gamma,r} \right] q \right] \det\left(\frac{\partial x_k}{\partial \eta_k} \right) r \right\}_p w_p$$

$$- \sum_{\substack{\text{all edges} \\ \text{on } C^+ + C^-}} \{ t_\gamma u_{\gamma,r} q r \} w + \sum_{\substack{\text{all} \\ \text{elements} \\ \text{in } A}} \sum_{p=1}^{4} \left\{ \left[\sigma_{\phi\phi} \frac{u_r}{r} - W \right] \det\left(\frac{\partial x_k}{\partial \eta_k} \right) q \right\}_p w_p. \tag{3.5}$$

Here r is the radial distance from the z-axis to the integration points.

3.2. Three-dimensional implementation

Consider a segment of the crack front, e.g. S_t as shown in Fig. 3. We take the limit $h \to 0$ to obtain the crack line identified by L_c. In the subsequent discussion we take L_c to be the line connecting the nodes $M-1$, M and $M+1$ as shown in Fig. 5, and identify the volume V with the collection of elements which contains the line L_c. Consistent with the isoparametric formulation, we take

$$q_i = \sum_{I=1}^{8} N_I Q_{iI} \quad i = 1, 2, 3 \tag{3.6}$$

where N_I are the trilinear shape functions and Q_{iI} are the nodal values for the I^{th} node. From the definition of q_k (see (2.15)), $Q_{iI} = 0$ if the I^{th} node is on S_1. For nodes inside V, Q_{iI} is given by interpolating between the nodal values on L_c and S_1; furthermore Q_{2I} vanishes identically.

Following standard manipulations,

$$\frac{\partial q_i}{\partial x_j} = \sum_{I=1}^{8} \sum_{k=1}^{3} \frac{\partial N_I}{\partial \eta_k} \frac{\partial \eta_k}{\partial x_j} Q_{iI} \tag{3.7}$$

where η_k are the coordinates in isoparametric space. Employing $2 \times 2 \times 2$ Gaussian integration, the discretized form for (2.17) is

$$\bar{J} = \sum_{\substack{\text{all} \\ \text{elements} \\ \text{in } V}} \sum_{p=1}^{8} \left\{ \left[\left(\sigma_{ij} \frac{\partial u_j}{\partial x_k} - W \delta_{ki} \right) \frac{\partial q_k}{\partial x_i} + \left(\alpha \sigma_{ii} \frac{\partial \theta}{\partial x_k} - f_i \frac{\partial u_i}{\partial x_k} \right) q_k \right] \det\left(\frac{\partial x_k}{\partial \eta_k} \right) \right\}_p w_p$$

$$- \sum_{\substack{\text{all faces} \\ \text{on } S^+ + S^-}} \left\{ t_i \frac{\partial u_i}{\partial x_k} q_k \right\} w \tag{3.8}$$

where $\bar{J}$ is the energy released for a unit virtual advance of a finite crack front segment. Here the quantities within $\{\ \}_p$ are evaluated at the 8 Gauss points and w_p and w are the respective weights. As discussed previously, the crack face traction contributions can be evaluated using the equivalent nodal forces and the spatial gradient of the nodal displacements, or using the standard integration procedure for boundary pressures [23].

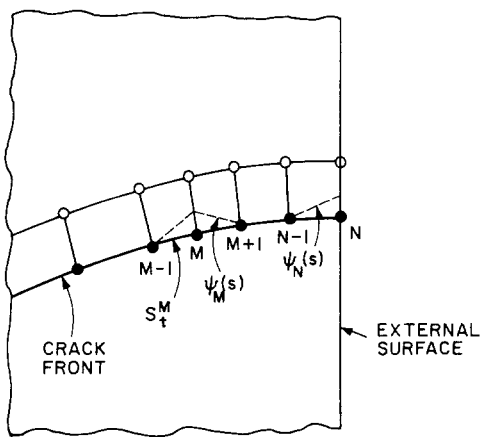

Figure 5. Schematic of the finite element mesh in the $x_1 - x_3$ plane illustrating the basis functions for an "interior" node and an "end" node along the crack front.

To construct the relationship between $J(s)$ and $\bar{J}$ we substitute (2.13) into (2.12) to get

$$\int_{L_c} J(s) l_j(s) m_j(s)\, \mathrm{d}s = \bar{J} \tag{3.9}$$

Now introduce piecewise continuous functions for $J(s)$ and $l_j(s)m_j(s)$.

Let J_K denote the value of $J(s)$ at the K^{th} node on the crack front and $\Psi_K(s)$ be linear piecewise basis functions defined along the crack front. Then

$$J(s) = \sum_{K=1}^{N} J_K \Psi_K(s) \tag{3.10}$$

where N is the total number of nodes on the crack front and

$$\Psi_K = \begin{cases} 1 & \text{at the } K^{\text{th}} \text{ node} \\ 0 & \text{at all other nodes.} \end{cases} \tag{3.11}$$

Similarly the function $l_j m_j$ in (3.9) can be represented by the same basis functions

$$l_j(s) m_j(s) = \sum_{J=1}^{N} L_J \Psi_J(s) \tag{3.12}$$

where L_J is the prescribed nodal value for the J^{th} node at the crack front.

Now direct attention to the particular node M on the crack front and make the convenient choice

$$L_J^M = \begin{cases} 1 & J = M \\ 0 & J \neq M \end{cases} \quad 1 \leqslant J \leqslant N \tag{3.13}$$

The crack front L_c^M is surrounded by the collection of elements which constitute V^M. By construction the only nodes along the crack which are members of V^M are the nodes $M-1$, M, and $M+1$ (or the nodes $N-1$ and N in the case of end segments, see Fig. 5). For this particular choice of L_J, q_i in V^M is given by (3.6), with Q_{iI} replaced by Q_{iI}^M. We take

$$Q_{iI}^M = m_i^M, \quad I = M \tag{3.14}$$

where m_i^M is the normal to the crack front (in the $x_1 - x_3$ plane of Fig. 3) at node M. The particular choice (3.14) may be interpreted as advancing the crack in the normal direction. At other nodes, Q_{iI}^M are obtained by interpolation subject to the restriction that the values on L_c^M (except for node M) and on S_1 are zero.

We evaluate $\bar{J}^M$ for the particular choice of L_J by substituting (3.6) and (3.7) with the appropriate Q_{iI}^M into (3.8) and carry out the integration as indicated. The outer summation only include the elements in V^M and the element faces on $S^+ + S^-$ defined by V^M. The results can be written as

$$\bar{J}^M = \sum_{I=1}^{U} \sum_{i=1}^{3} B_{iI} Q_{iI}^M \tag{3.15}$$

where U is the number of nodes in V^M and B_{iI} are the contributions from the field quantities associated with the I^{th} node in V^M; note that $Q_{2I}^M \equiv 0$. Expression (3.15) indicates the linear dependence of $\bar{J}^M$ on Q_{iI}^M.

To obtain an explicit expression for the nodal values J_K, we substitute (3.10) and (3.12) into the left hand side of (3.9) and then use (3.13) to get

$$\sum_{K=1}^{N} J_K \int_{L_c} \Psi_M(s) \Psi_K(s)\, \mathrm{d}s = \bar{J}^M. \tag{3.16}$$

Here the integration need only be carried out over the part of the crack front length L_c where $\Psi_M(s)$ is nonzero. The resulting expression can be written as

$$\sum_{K=1}^{N} A_{MK} J_K = \bar{J}^m \tag{3.17}$$

where A_{MK} is the coefficient for the K^{th} node and is nonzero only for nodes on L_c^M.

By repeating the above process for every node on the crack front, we obtain a linear system of N equations with N unknowns J_K. For the particular choice of basis functions, A_{MK} has a bandwidth of 3. The pointwise energy release rate is obtained by substituting the solution for J_K into (3.10). The nodal value J_M can also be obtained directly using (2.18), i.e.,

$$J_M = \frac{\bar{J}^M}{\int_{L_c^M} \Psi_M(s)\, ds}. \tag{3.18}$$

the relative merits of the methods based on (3.17) and (3.18) for computing the (pointwise) values of the energy release rate at the crack front nodes are briefly discussed in Section 4.3.

4. Finite element thermo-mechanical crack analyses

To illustrate the use of the domain integrals and to examine the accuracy of the domain method, the plane strain crack problem analyzed by Wilson and Yu [16] is selected as the benchmark problem. An edge cracked strip with crack length a is subject to a linear temperature variation through the width, W, with zero temperature at mid-width, and temperature $\pm\theta_e$ at the right and left edges. The crack geometry and the finite element mesh of the upper half geometry is shown in Fig. 6. The "rectangular" mesh design has 20 elements across the width and 12 elements along the height; all elements are 4-node isoparametric elements. The first integration domain is comprised of the two elements

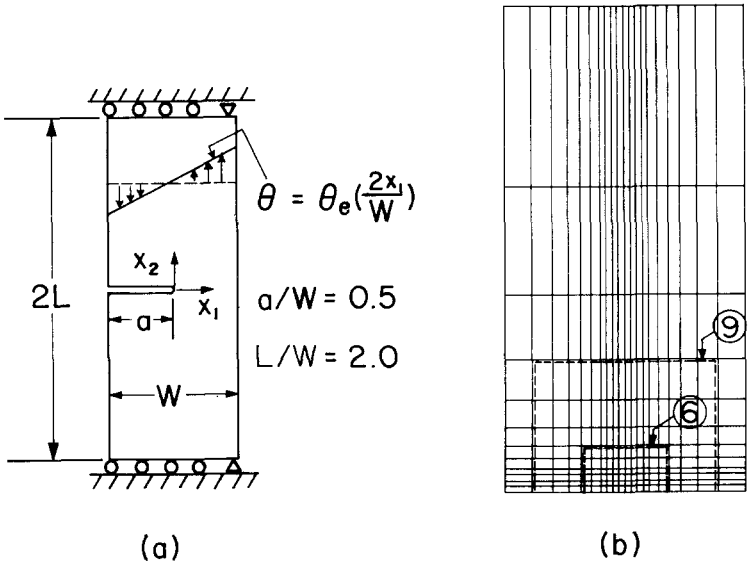

Figure 6. (a) Edge cracked strip subject to thermal field. (b) Finite element mesh of the upper-half geometry. The boundaries of the integration domains 6 and 9 are indicated.

adjoining the crack tip; the second domain, which includes the first domain and the adjoining layer of elements, has eight elements. Domains three through nine are also put together in this fashion. The boundaries of the sixth and ninth integration domains are indicated in Fig. 6. Elastic and elastic-plastic analyses to be discussed in the subsequent sections are carried out with the ABAQUS (copyright) finite element program. The calculations for the energy release rate (J values) according to the domain formulae (3.4), (3.5) and (3.8) are carried out in a separate post-processing program.

4.1. Thermo-elastic analysis

Under plane strain conditions, the stress (due to the thermal field) at the right edge of the uncracked strip is $\sigma_\theta = E\alpha\theta_e/(1-\nu)$; ν is taken to be 0.3 in the calculations. The values of J as calculated by the discrete domain formula (3.4) for the various domains are listed in the second and third columns in Table 1. Here J is normalized by $\sigma_\theta^2 a/E$. Under plane strain elastic conditions, the stress intensity factor K_I and J are related by $K_I = [JE/(1-\nu^2)]^{1/2}$. The values of K_I normalized by $\sigma_\theta(\pi a)^{1/2}$ are also listed; the normalized K_I values do not depend on ν. The average value is within 4 percent of Wilson and Yu's value. They employed a mesh which is coarser than ours. Indeed using a coarser mesh we obtained K_I values which are within 1 percent of their values. We also observed that the variation in the computed K_I values from one domain to another is smaller than 1 percent if the near-tip domain (the first domain) is excluded. For this particular exercise we did not surround the crack tip with ($1/\sqrt{r}$ singular) crack-tip elements. It is well-known that the accuracy of K_I (or J in nonlinear analysis) values obtained from near-tip domains can be considerably improved if the proper near-tip mesh design an crack tip elements are employed in the crack tip region [2,4,7,19].

To examine the accuracy of the computed results when the source of loading is crack face traction, we analyze the same geometry for $\theta = 0$ everywhere, and loading the strip by crack face traction. To enable a direct comparison with the preceding thermal stress calculations, we apply crack face traction which is the negative of the traction along the prospective crack plane in the uncracked geometry due to the thermal field shown in Fig. 6. By the principle of linear superposition, K_I due to the thermal field is the same as K_I due to the crack face traction.

The J values calculated using (3.4) and the normalized K_I values are listed in the last

Table 1. Stress intensity factors calculated by the domain integral method

Domain	Thermal stress problem		Equivalent problem by crack face traction	
	$J/(\sigma_\theta^2 a/E)$	$K_I/\sigma_\theta(\pi a)^{1/2}$	$J/(\sigma_\theta^2 a/E)$	$K_I/\sigma_\theta(\pi a)^{1/2}$
1	0.6366	0.4719	0.6408	0.4734
2	0.6618	0.4811	0.6900	0.4913
3	0.6712	0.4845	0.6923	0.4921
4	0.6759	0.4862	0.6954	0.4932
5	0.6800	0.4877	0.7004	0.4950
6	0.6827	0.4887	0.7033	0.4960
7	0.6848	0.4894	0.7113	0.4988
8	0.6869	0.4902	0.7253	0.5037
9	0.6899	0.4912	0.7503	0.5123
Average value	0.6744	0.4857	0.7010	0.4951
Average value from [16]		0.5035		0.5043

two columns in Table 1. Again the calculated values show little variation from one domain to another and are also remarkably close to the thermal stress results. We add that the crack face contributions to (3.4) are computed by using the equivalent nodal forces and the nodal displacement gradients.

At this juncture we note that in the preceding calculations, a "pyramid" q_1 function has been employed, i.e., $q_1 = 1$ at the crack tip, $q_1 = 0$ on the edge of the domain and q_1 varies linearly between the peak and the rectangular edges. In this sense an equal weighting has been applied to the energy-momentum tensor while the body force, thermal contributions and crack face tractions have been linearly weighted (see (2.10) and (3.4)). If the accuracy of the calculated finite element fields over the entire geometry is comparable, then the calculated J values will be insensitive to the size and shape of the domain and the choice of a q_1 function. In general, the numerical resolution of the near-tip fields is less accurate than the numerical resolution of the remote fields. These considerations should be taken into account in selecting the domain of integration and a q_1 function. Needless to say, using several different domains for the purpose of establishing a domain-independent value can serve as a useful check on the crack analysis.

4.2. Thermo-elastic-plastic analysis

The thermal crack problem examined in Section 4.1 is reanalyzed using a J_2 flow theory equivalent of the constitutive relations (2.5)–(2.7). The analysis employs a piecewise power law hardening representation where the uniaxial stress-strain relation in the plastic range is given by $\epsilon/\epsilon_0 = (\sigma/\sigma_0)^n + \alpha\theta/\epsilon_0$ where ϵ_0 and σ_0 are the yield strain and stress respectively. We take the strain hardening exponent n to be 10 and ν to be 0.3. The mesh shown in Fig. 6 is employed in this analysis.

To study the effect (if any) of the choice of a q_1 function on the calculated J values, we present J values extracted by using a "pyramid" q_1 function (which has been used in

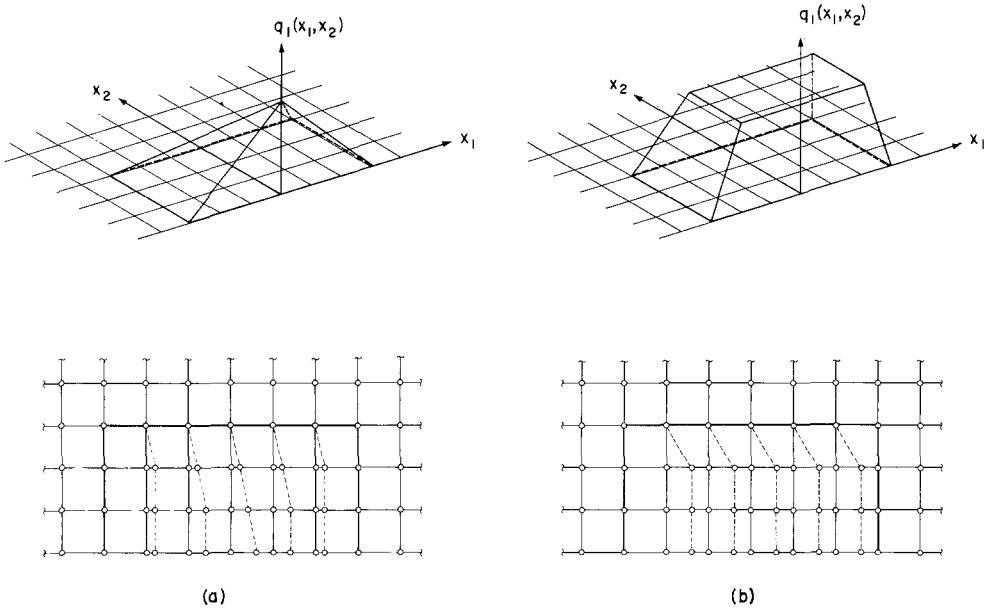

Figure 7. (a) "Pyramid" q_1 function and its interpretation as a translation in the x_1 direction (b) "Plateau" q_1 function and its interpretation as a translation in the x_1 direction.

Table 2. Normalized J values at two temperatures calculated by the domain integral method

Domain	$\epsilon_\theta/\epsilon_0 = 1$		$\epsilon_\theta/\epsilon_0 = 2$	
	Pyramid q_1 function	Plateau q_1 function	Pyramid q_1 function	Plateau q_1 function
	$J/(\sigma_0\epsilon_0 a)$	$J/(\sigma_0\epsilon_0 a)$	$J/(\sigma_0\epsilon_0 a)$	$J/(\sigma_0\epsilon_0 a)$
1	1.2532	1.2532	3.8901	3.8901
2	1.3363	1.4195	4.1558	4.4216
3	1.3682	1.4321	4.2341	4.3906
4	1.3862	1.4400	4.2670	4.3657
5	1.4019	1.4419	4.2921	4.3631
6	1.4124	1.4434	4.3025	4.3383
7	1.4208	1.4463	4.3020	4.2994
8	1.4282	1.4506	4.2853	4.2168
9	1.4172	1.3756	4.2334	4.0373
Average value	1.3805	1.4114	4.2180	4.2581

the preceding calculations) as well as a "plateau" q_1 function. The "plateau" q_1 function has a value (or height) of unity everywhere in the domain except in the outermost ring of elements. Here the value (or height) decreases linearly from unity to zero within one element width. The "pyramid" and "plateau" q_1 function together with the virtual crack extension interpretation of q_1 as a translation in the x_1 direction is depicted in Fig. 7. It may be noted that in the subdomain where q_1 is constant (corresponding to a rigid translation of the subdomain in the context of the virtual crack extension technique) there

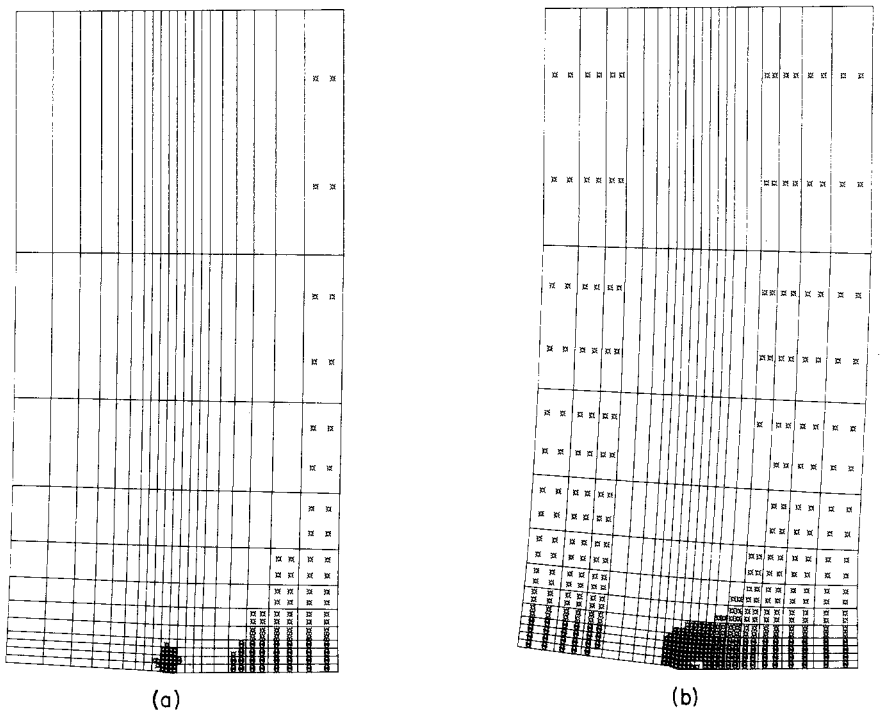

Figure 8. (a) Plastic zone at temperature gradient corresponding to $\theta_e = \epsilon_0/\alpha$ (b) Plastic zone at temperature gradient corresponding to $\theta_e = 2\epsilon_0/\alpha$.

is no contribution from the Eshelby energy-momentum tensor to the domain integral (see (2.10) and (3.14)).

In the analysis the temperature gradient in the strip is raised to the intermediate value corresponding to $\theta_e = \epsilon_0/\alpha$ in two increments and to the final value of $\theta_e = 2\epsilon_0/\alpha$ in another eight increments. At each increment two or three equilibrium iterations are applied. The normalized J values are tabulated in Table 2. We note that the near-tip J values deviated from the consensus values. This deviation is expected since the near-tip mesh design is not suited for providing an accurate resolution of the near-tip fields. J values from domain 9, which includes elements with relatively large aspect ratios, also deviated from the consensus value. However the adverse mesh effects appeared to be mitigated by the choice of a smoother q_1 function, e.g., the J values extracted from domain 9 using the "pyramid" function is very nearly equal to the consensus values. In addition to the "pyramid" and "plateau" q_1 functions, we also experimented with "cone" and "dome" q_1 functions. We observe that the J values extracted from moderately-sized domains (e.g., domains 2 to 8) are insensitive to the choice of q_1 functions. The domain independent J values also suggest that the loading induced by the temperature field is (nearly) proportional.

The plastic zones for the two temperature levels are shown in Fig. 8. At the lower temperature, an isolated plastic zone develops at the crack tip while at the right edge of the strip the plastic zone has spread along the entire length. At the higher temperature, the two plastic zones merged into one; in addition the left edge of the strip has also yielded. The yielding at the left edge is caused by the plane strain constraint which elevates the through thickness stress to levels much higher than the in-plane stresses.

A plot of the variation of the computed J with the increase of the thermal strain ϵ_θ defined by $\epsilon_\theta = \alpha\theta_e$ is shown in Fig. 9. For comparison, the elastic curve is also included.

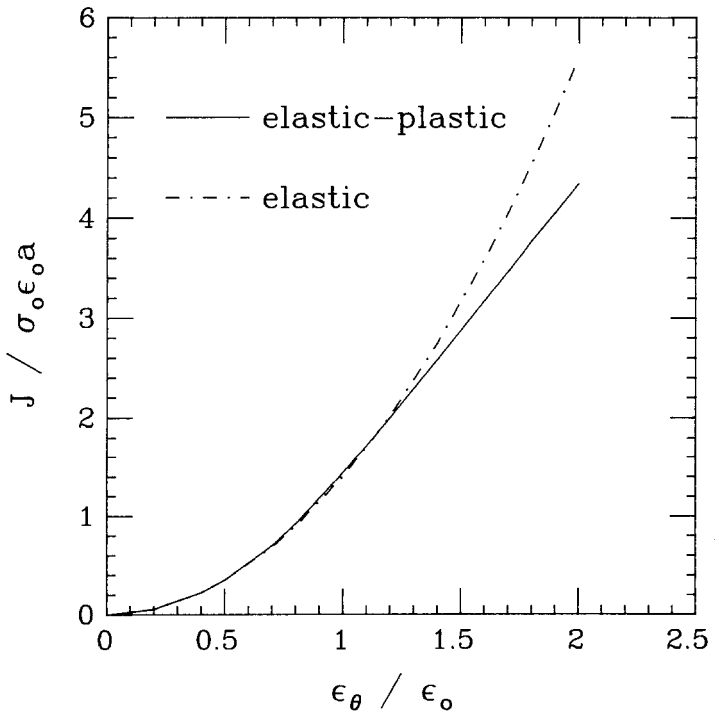

Figure 9. Variation of J with respect to increasing thermal strain for an elastic and elastic-plastic solid.

We observe that the effect of plasticity is to lower the J values. This effect is expected for a deformation constrained thermally stressed body.

4.3. 3-dimensional thermo-elastic analysis

The temperature field $\theta(x_1, x_2, x_3) = \theta_e(2x_1/W)$ is imposed on the 3-D cracked slab depicted in Fig. 10a; the end faces of the slab at $x_2 = \pm L$ are constrained against motion in the x_2 direction. The finite element model of the quarter-body is shown in Fig. 10b; the model is generated by repeating the planar mesh of Fig. 6b on the planes $x_3/B = 0.0$, 0.52, 0.78, 0.90, 0.95, 0.975, 0.99, 1.0. Thus the model has 7 layers of 8-node brick elements across the half-thickness and each layer has 240 elements. Using the convention discussed earlier (see Fig. 2), the normalized distance along the crack front x_3/B is denoted by s. We briefly discuss the setting up of the integration domains for calculating J associated with a unit virtual advance of a finite crack front segment (e.g. see Fig. 5).

Consider the node identified by its position s_M along the crack front (M can range from 1 to N; N being the number of nodes on the crack front). We direct our attention to the two layers of elements between the planes $x_3/B = s_{M-1}$ and $x_3/B = s_{M+1}$ (one layer of elements in the case of the node s_1 on the mid-plane and s_N on the free surface). The first integration domain is comprised of the 4 brick elements adjoining the crack front node s_M. The second domain is obtained by adding one "ring" of elements around the first domain; thus the second domain has a total of 16 brick elements. In this manner the integration domains 3 through 9 are put together. These integration domains are the 3-D equivalents of the 2-D integration domains for the plane strain problem depicted in Fig. 6b.

The variation of q and in particular the nodal values Q within the integration domain are generated in the following manner. First we prescribe q_2 and q_3 to be zero everywhere since the normal to the crack front is in the x_1 direction. On the plane $x_3/B = s_M$ (this plane contains the node s_M), the variation of q_1 is given by the plateau function as

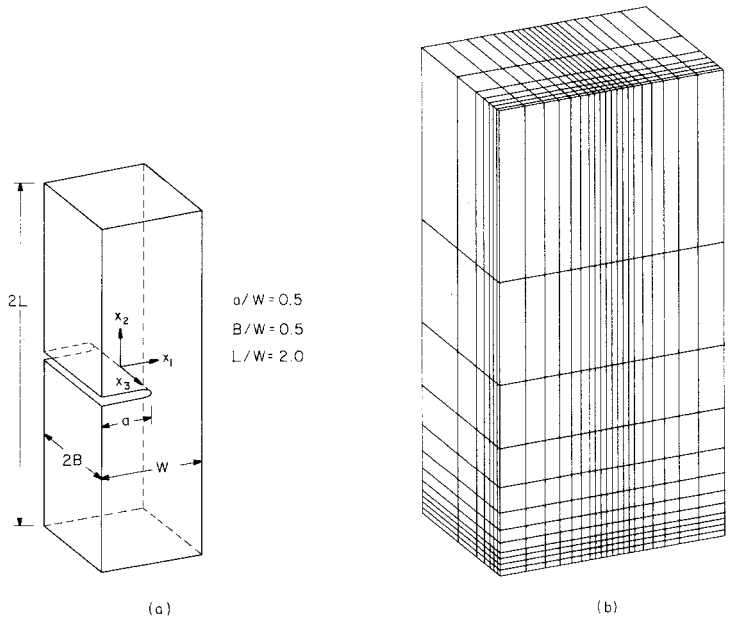

Figure 10. (a) Schematic of cracked slab. (b) Finite element mesh of quarter-body.

Table 3. Variation of(pointwise) energy release rate along crack front

Domain	$J(s)/J_{\text{plane strain}}$							
s	0.000	0.520	0.780	0.900	0.950	0.975	0.990	1.000
1	0.502	0.491	0.448	0.394	0.344	0.304	0.267	0.172
2	0.540	0.528	0.482	0.422	0.368	0.323	0.280	0.182
3	0.540	0.531	0.485	0.425	0.369	0.323	0.280	0.186
4	0.538	0.531	0.487	0.425	0.369	0.323	0.280	0.188
5	0.535	0.532	0.489	0.425	0.369	0.323	0.281	0.194
6	0.531	0.534	0.492	0.425	0.368	0.324	0.281	0.200
7	0.528	0.537	0.494	0.424	0.369	0.325	0.283	0.210
8	0.526	0.540	0.495	0.424	0.370	0.327	0.285	0.221
9	0.533	0.546	0.499	0.431	0.380	0.338	0.296	0.206
Average value	0.530	0.530	0.486	0.422	0.367	0.323	0.281	0.195

depicted in Fig. 7b. On the boundary planes $x_3/B = s_{M-1}$ and $x_3/B = s_{M+1}$, q_1 is accordingly prescribed to vanish. With this information in hand the q_1 values at the nodes (within the integration domain) denoted by Q_{iI}'s are thus known. The variation of q_1 and $\partial q_1/\partial x_i$ within an element is given by (3.6) and (3.7) respectively.

We calculate the nodal values J_K using two methods, the method identified with (3.17) and the simpler method identified with (3.18). The values J_K determined by the first method differed only slightly from the values determined by the second method; the difference being less than 3% over the crack front $0 \leqslant s \leqslant 0.98$. However, the J values at the outermost node ($s = 1$) can differ by as much as 25%. This is not surprising since $J(s)$ drops rather sharply as the free surface is approached. The resolution difficulty is compounded by the skewness of the outermost layer of elements. With method (3.17), the loss of accuracy at the last node has a slight effect on the accuracy of the J values at the neighboring nodes. This accuracy loss is confined to the last nodal value in method (3.18). In the next paragraph, the J values determined by the latter method are discussed.

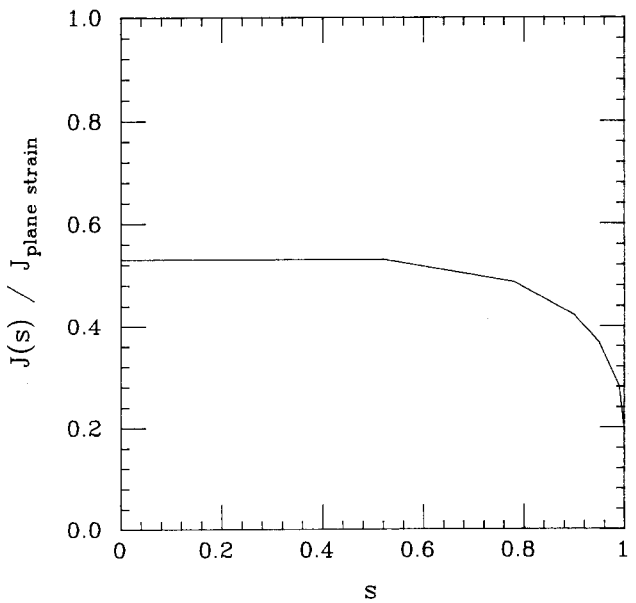

Figure 11. Variation of (pointwise) energy release rate along crack front.

The pointwise value of the energy release rate $J(s)$ normalized by the corresponding plane strain value is given in Table 3 at 8 distinct values of s (these are the locations of the 8 nodes on the crack front). The somewhat larger variation of J at $s = 1.0$ (intersection of crack front with external surface) is not unexpected since the outermost layer of elements have very large aspect ratios. Discounting this mesh problem, $J(s)$ extracted from domains 2 through 8 at the other 7 crack front locations are essentially domain independent. The average values are plotted in Fig. 11.

Similar variations of $J(s)$ along the crack front of a compact specimen have been reported in [27]. Nevertheless there is an important difference. The ratio $J(s)/J_{\text{plane strain}}$ is slightly larger than unity over a large portion of the crack front ($0 \leqslant s \leqslant 0.7$) of a typical compact specimen. For the thermally loaded cracked slab this ratio is about 0.5. The example problem serves to point out that three-dimensional effects on the intensity of near-tip stress and deformation are dependent on the "source" of the loading (e.g. thermal vs. mechanical loading).

5. Discussion

The objective of the paper is to demonstrate the viability of the domain integral method for calculating the pointwise energy release rate under thermal-mechanical loading. To this end, we outlined the numerical implementation for the 4-node quadrilateral and the 8-node brick elements; the implementation for higher order elements follows along exactly the same lines and has been discussed in [7] in the context of isothermal analysis. The example problems were carried out to illustrate the use of finite domain integrals and some aspects of accuracy; the 4/8 node element models served the purpose. While we did not carry out numerical experimentations specific to the thermal stress problem using higher order elements, our earlier studies suggest that the 9/27 node 2D/3D Lagrangian elements in conjunction with selective/reduced integration are better suited for elastic-plastic and fully plastic problems where the incompressible plastic deformation dominates the structural behavior [21,22].

There is also ample evidence which indicates that 8/20 node 2D/3D elements with selective/reduced integration are suited for elastic-plastic problems; nevertheless their usefulness for full plastic problems (e.g. [7,22]) have not been investigated. An aspect of nonlinear analysis which is frequently overlooked is the adequacy of the mesh design. A good mesh design must have the ability to resolve the overall and local deformation pattern particular to the nonlinear problem. In connection with this point, we note that more accurate J values could have been extracted from the crack tip domain if singular elements of the type advocated in [19,22,7] were used in the example problems discussed in Section 4. The effect of near-tip element choice and mesh design on the accuracy of plane strain fully plastic crack solutions is discussed in [7,22].

We have focussed on solids characterized by a path-independent deformation theory of plasticity. The (area/volume) domain integral method can also be employed in crack analyses, when the solid is characterized by an incremental theory of plasticity, if the strain energy density W is replaced by the load-path dependent stress work density W^I. The integration for W^I follows the actual strain trajectory (and temperature history) of a material point. For incremental plasticity, the interpretation of J (or $J(s)$) as the energy release rate cannot be made. Nonetheless, many studies have demonstrated that if the applied loads/displacements are monotonically increasing and if the stress histories for material particles near the crack tip are nearly proportional, then the value of J provides a measure of the intensity of the near-tip stresses and deformation. It is this role that is pertinent to elastic-plastic fracture mechanics and considerable analytical, numerical and experimental investigations have shown that the value of J is a relevant characterizing

parameter of the near-tip fields when certain size requirements are met (see [1,24]).

With the usual reinterpretations the domain integral definitions of J (2.10), (2.17) and (2.20) are also applicable to deformations of arbitrary magnitude. Here the area/volume domain, boundaries defined by contours/surfaces and associated normal vectors are taken in the undeformed configuration. The stresses are replaced by the nominal (transpose of the first Piola-Kirchhoff) stress tensor, displacement gradients are re-expressed in terms of the deformation gradient, and W is interpreted as the strain energy per unit undeformed volume [14,2].

The domain integral expression for the energy release rate is naturally compatible with the finite element solution process and in this sense is more naturally tied to the energy variational statement of equilibrium than the line-integral expression (2.2) and the corresponding surface-integral expression for the 3-D cracked body [15]. In particular the finite element implementation of (2.10) and (2.17) is most conveniently carried out using the specially chosen global orthogonal Cartesian coordinate system such that the x_2 coordinate is orthogonal to the crack plane as described in Section 2 (also see [7]). Should another Cartesian system be adopted, the fields and quantities in (2.10) and (2.17) can be obtained by the usual tensor transformations. Alternatively, we could treat the energy release rate expression (2.2) as the J_1 component of a vector integral. Indeed some investigators choose to write (2.10) and (2.17) using fields and quantities defined with respect to a global coordinate system arbitrarily oriented with respect to the crack plane. In this case the energy release rate J for the crack extending in its own plane is the scaled sum of its components (J_1, J_2, J_3) (see [15]).

Ackowledgement

The authors are grateful for the support from the U.S. Department of Energy through Grant DE-AC02-80-ER10556 and the Materials Research Laboratory at Brown University funded by the National Science Foundation. We are pleased to acknowledge the support of the ABAQUS finite element program provided by Hibbitt, Karlsson and Sorensen, Inc., Providence, Rhode Island. Appendix B is the result of a discussion with Professor B. Storåkers of the Royal Institute of Technology, Stockholm, Sweden.

The computations reported here were carried out on a VAX-11/780 computer at Brown University, Division of Engineering, Computational Mechanics Computer Facility. This facility was made possible by grants from the U.S. National Science Foundation (Grant ENG78-19378), the General Electric Foundation and the Digital Equipment Corporation.

Appendix A

A.1. A note on J as an amplitude parameter for the crack tip singular fields

The form of the energy release rate J for quasi-static isothermal conditions is given by (2.2) as

$$J = \lim_{\Gamma \to 0} \int_{\Gamma} [W\delta_{1i} - \sigma_{ij} u_{j,1}] n_i \, \mathrm{d}C. \tag{A.1}$$

The above result is solely a consequence of mechanical energy balance. In the particular context of an uncoupled thermo-mechanical theory (deformation theory solid) (A.1) is still valid since the thermal strains are bounded. In this case the strain energy $W = W(\epsilon_{ij}, \theta)$ is given by (2.7).

An important additional role of J is as an amplitude parameter for the crack tip singular fields, i.e. a measure of the intensity of the near tip deformation. This is a well known result for the isothermal analysis of deformation theory solids. In the presence of thermal strains (uncoupled theory) the same interpretation can be made since the temperature is non-singular and the crack tip singularity is unaffected by the bounded thermal strains. To demonstrate this, the standard argument presented for the isothermal case in [1], is reproduced. We

take Γ to be a circular contour centered at the crack tip. If J is to be nonvanishing (recall that J is the energy released per unit crack advance) then the integrand in (A.1) must be of order r^{-1} and therefore, noting that $r \to 0$ is implied in (A.1),

$$r\left[W\delta_{1i} - \sigma_{ij}u_{j,1}\right]n_i = f(\zeta) \quad \text{as } r \to 0. \tag{A.2}$$

An expression for J may then be written as

$$J = \int_{-\pi}^{\pi} f(\zeta)\, \mathrm{d}\zeta \tag{A.3}$$

and thus J is seen to be related to the near tip deformation fields. From (A.2) and (A.3) it is clear that

$$W \sim J/r. \tag{A.4}$$

Now consider a uniaxial power-law relation of the form

$$\epsilon/\epsilon_0 = \sigma/\sigma_0 + \gamma(\sigma/\sigma_0)^n + \alpha\theta/\epsilon_0. \tag{A.5}$$

Noting that the thermal strains are bounded, the nonlinear term $(\sigma/\sigma_0)^n$ will dominate the material response as $r \to 0$. It then follows from (A.4) and a J_2 generalization of (A.5) that the following asymptotic crack tip relations must hold

$$\sigma_{ij} \sim \left(\frac{J}{r}\right)^{1/(n+1)}, \quad \epsilon_{ij} \sim \left(\frac{J}{r}\right)^{n/(n+1)}. \tag{A.6}$$

The above result illustrates the role played by J as a measure of the intensity of the crack tip singularity fields.

The dual role of J as the energy release rate and a measure of the crack tip deformation has been illustrated. The asymptotic behavior of the terms which contribute to (A.1) and in particular the boundedness of the temperature field θ are central to the latter interpretation. It is clear from the above considerations that (A.1) is necessarily the starting point for the derivation of a finite domain integral representation of the energy release rate as described in the text. It also follows from (A.1) that (as summarized in (A.2)–(A.6)) J is the amplitude of the crack tip singularity fields. We emphasize that in the presence of thermal strains J is only defined by the limiting contour $\Gamma \to 0$ and the resulting domain integral must include the near crack tip region $r \to 0$.

Appendix B

B.1. Derivation of $J(s)$ for sharp crack configuration

A concise derivation of a finite domain (i.e. volume) integral expression for the energy release rate along a three-dimensional crack front in a thermo-mechanical field has been presented in Section 2. The derivation is somewhat heuristic with nonessential manipulations being omitted for the sake of clarity and physical interpretation. Attention was confined to a notch, with thickness h, and it was argued that the sharp crack configuration of interest is attained in the limit as $h \to 0$. In this appendix we consider a mathematically sharp crack from the outset and give an alternative derivation of the expression for the pointwise energy release rate $J(s)$. We also show how the axisymmetric and two-dimensional specializations may be readily derived from the three-dimensional result.

The pointwise energy release rate at the point s of a curved crack front with in-plane normal $\nu_k(s)$ is given by the generalization of (2.2) as

$$J(s)\nu_k(s) = \lim_{\Gamma \to 0} \int_{\Gamma(s)} \left[\sigma_{ij}u_{j,k} - W\delta_{ik}\right]m_i\, \mathrm{d}C. \tag{B.1}$$

Here Γ is the circular contour in the plane normal to the crack front, * as depicted in Fig. 1 for the case where the in-plane normal to the crack front coincides with the x_1 axis, and m_1 is the normal to the contour Γ pointing away from the body i.e. $m_i = -n_i$ on Γ. The energy released when a finite segment, L_c, of the crack front advances in amount $\Delta a l_k(s)$ is given by (2.12)

$$\bar{J}\Delta a = \Delta a \int_{L_c} J(s) l_k(s) \nu_k(s)\, \mathrm{d}s. \tag{B.2}$$

On employing (B.1) in (B.2) we obtain

$$\begin{aligned}\bar{J} &= \int_{L_c} l_k(s) \left[\lim_{\Gamma \to 0} \int_{\Gamma(s)} \left(\sigma_{ij}u_{j,k} - W\delta_{ik}\right)m_i\, \mathrm{d}C\right] \mathrm{d}s \\ &= \lim_{\Gamma \to 0} \int_{S_t} \left[\sigma_{ij}u_{j,k} - W\delta_{ik}\right] l_k m_i\, \mathrm{d}S.\end{aligned} \tag{B.3}$$

* The crack front is defined as the line formed by the intersection of the crack faces.

For the sharp crack configuration being considered here S_t is the 'tubular' surface enclosing the crack front segment and the limiting process consist of shrinking the 'tube' radius to zero. This expression may be conveniently written as

$$\bar{J} = -\lim_{\Gamma \to 0} \int_{S_t} l_k H_{ki} m_i \, \mathrm{d}S \tag{B.4}$$

where

$$H_{ki} = W\delta_{ki} - \sigma_{ij} u_{j,k} \tag{B.5}$$

contains the energy contributions to the integral over S_t. If inertia cannot be neglected or if the heat flux is not bounded these terms (and any other 'sources of energy') can be appropriately incorporated in the definition of H_{ki}. Note that for a nonlinear elastic solid under quasistatic isothermal conditions $H_{ki} = P_{ki}$, Eshelby's elastic energy-momentum tensor. Under certain circumstances the energy-momentum tensor is divergence free i.e. $P_{ki,i} = 0$ indicating a conserved quantity and indeed path independence of the J-integral is a well known consequence of this result. In the general case of thermomechanical loading and with the existence of body forces and crack face tractions the divergence of H_{ki} does not vanish and J is only defined by the limiting contour $\Gamma \to 0$.

For the general case considered above the divergence of H_{ki} is nonvanishing and we can write

$$H_{ki,i} = h_k \quad \text{in } V \tag{B.6}$$

where V is any subregion of the body not containing a singularity and the exact form of h_k depends on the form of H_{ki} and will be identified later for the thermo-mechanical analysis of the present discussion. We take the inner product of (B.6) with an arbitrary vector field q_k and integrate over the volume V to give

$$\int_V H_{ki,i} q_k \, \mathrm{d}V = \int_V h_k q_k \, \mathrm{d}V.$$

With standard manipulations and application of the divergence theorem we obtain

$$\int_S q_k H_{ki} m_i \, \mathrm{d}S = \int_V (H_{ki} q_{k,i} + h_k q_k) \, \mathrm{d}V \tag{B.7}$$

where it has been assumed that q_k is smooth enough for the indicated operations to be carried out. Now if we identify the arbitrary closed surface S with the surface $S_1 + S^+ + S^- - S_t$ as shown in Fig. 3a (for the case of a notch)

$$q_k = \begin{cases} l_k \text{on } S_t \\ 0 \text{ on } S_1 \\ \text{otherwise arbitrary} \end{cases}$$

then on rearrangement and noting (B.4) we can write (B.7) as

$$\bar{J} = -\int_V (H_{ki} q_{k,i} + h_k q_k) \, \mathrm{d}V + \int_{S^+ + S^-} q_k H_{ki} m_i \, \mathrm{d}S. \tag{B.8}$$

The last term consists of the contribution due to crack face tractions. The expression (B.8) is the equivalent of (2.17), where it only remains to identify the quantities H_{ki} and h_k for the case of a thermally stressed body.

Equating (B.2) and (B.8) an expression involving the pointwise energy release rate, $J(s)$ as the only unknown is obtained. To a first approximation $J(s)$ may be assumed constant over the length L_c and brought outside the integral sign in (B.2) to yield

$$\bar{J} = J(s) \int_{L_c} l_k(s) \nu_k(s) \, \mathrm{d}s = -\int_V (H_{ki} q_{k,i} + h_k q_k) \, \mathrm{d}V + \int_{S^+ + S^-} q_k H_{ki} m_i \, \mathrm{d}S \tag{B.9}$$

or

$$J(s) = \bar{J} / \int_{L_c} l_k \nu_k \, \mathrm{d}s. \tag{B.10}$$

It is useful to write these results in invariant form for subsequent interpretation, i.e.,

$$\bar{J} = -\int_V (\nabla \boldsymbol{q} : \boldsymbol{H} + \boldsymbol{q} \cdot \boldsymbol{h}) \, \mathrm{d}V + \int_{S^+ + S^-} \boldsymbol{q} \cdot \boldsymbol{H} \cdot \boldsymbol{m} \, \mathrm{d}S, \quad J(s) = \bar{J} / \int_{L_c} \boldsymbol{l} \cdot \boldsymbol{\nu} \, \mathrm{d}s. \tag{B.11}$$

B.2. Axisymmetric and two-dimensional specializations

The results (B.11) can be readily specialized for the case of an axisymmetric crack configuration. We consider a local set of cylindrical polar coordinates at each point on the crack front. In the $r - z$ plane the surfaces S_1, S^+

and S^- reduce to the curves C_1, C^+ and C^- respectively while the surface S_t becomes the curve Γ. The area enclosed by C_1 is denoted A and an element of area $dA = dr\,dz$ (see Fig. 4c). Using these definitions and the axisymmetry of the problem $(B.11)_1$ can be written

$$\bar{J} = -2\pi\int_A (\nabla \boldsymbol{q} : \boldsymbol{H} + \boldsymbol{q}\cdot\boldsymbol{h})\, r\, dA + 2\pi\int_{C^+ + C^-} \boldsymbol{q}\cdot\boldsymbol{H}\cdot\boldsymbol{m} r\, dC. \tag{B.12}$$

We now note that for uniform radial expansion of the axisymmetric crack $\boldsymbol{l} = \boldsymbol{e}_r$ and a suitable choice of the vector $\boldsymbol{q}$ is therefore $\boldsymbol{q} = q(r, z)\boldsymbol{e}_r$ where

$$q(r, z) = \begin{cases} 1 & \text{on } S_t \text{ i.e. on } \Gamma \\ 0 & \text{on } S_1 \text{ i.e. on } C_1 \\ \text{otherwise arbitrary} & \end{cases}$$

Letting the Greek indices β and γ range over the coordinates r and z the above expression (B.12) can be expanded (using (B.5)) to yield

$$\bar{J} = 2\pi\int_A \left[\left(\sigma_{\gamma\beta} u_{\gamma,r} - W\delta_{r\beta}\right) r q_{,\beta} + \left(\frac{u_r}{r}\sigma_{\phi\phi} - W\right) q - r h_r q \right] dA - 2\pi\int_{C^+ + C^-} t_\gamma u_{\gamma,r} q r\, dC \tag{B.13}$$

where $h_r = \boldsymbol{e}_r\cdot\boldsymbol{h}$ and $\sigma_{\phi\phi}$ is the hoop stress. We note $\boldsymbol{\nu} = \boldsymbol{e}_r$ and L_c is the circular crack front of radius R hence

$$\int_{L_c} \boldsymbol{l}\cdot\boldsymbol{\nu}\, ds = 2\pi R \tag{B.14}$$

and the pointwise energy release rate $J = J(s)$ is given by $(B.11)_2$ as

$$J = \frac{\bar{J}}{2\pi R} = \frac{\tilde{J}}{R}. \tag{B.15}$$

The specialization of the expression $(B.11)_1$ to the case of a plane strain line crack oriented along the x_1 axis (i.e. a straight crack front with in-plane normal $\boldsymbol{e}_1$) is similar to that of the previous section. Referring to Fig. 1 an element of area is now given by $dA = dx_1\,dx_2$ and the expression $(B.11)_1$ is written (for length L of crack front)

$$\bar{J} = -L\int_A (\nabla \boldsymbol{q} : \boldsymbol{H} + \boldsymbol{q}\cdot\boldsymbol{h})\, dA + L\int_{C^+ + C^-} \boldsymbol{q}\cdot\boldsymbol{H}\cdot\boldsymbol{m}\, dC, \tag{B.16}$$

Now noting that $\boldsymbol{l} = \boldsymbol{e}_1$ a suitable choice of the vector $\boldsymbol{q}$ is therefore $\boldsymbol{q} = q(x_1, x_2)\boldsymbol{e}_1$ where

$$q(x_1, x_2) = \begin{cases} 1 & \text{on } S_t \text{ i.e. on } \Gamma \\ 0 & \text{on } S_1 \text{ i.e. on } C_1 \\ \text{otherwise arbitrary} & \end{cases}$$

The expression (B.16) can be expanded to yield

$$\bar{J} = L\int_A \left[\left(\sigma_{ij} u_{j,1} - W\delta_{1i}\right) q_{,i} - h_1 q \right] dA - L\int_{C^+ + C^-} t_i u_{i,1} q\, dC \tag{B.17}$$

where $h_1 = \boldsymbol{e}_1\cdot\boldsymbol{h}$. Here $\boldsymbol{\nu} = \boldsymbol{e}_1$ and L_c is the length L of the crack front hence

$$\int_{L_c} \boldsymbol{l}\cdot\boldsymbol{\nu}\, ds = L \tag{B.18}$$

and the pointwise energy release rate $J = J(s)$ is given by $(B.11)_2$ as

$$J = \frac{\bar{J}}{L} = \int_A \left[\left(\sigma_{ij} u_{j,1} - W\delta_{1i}\right) q_{,i} - h_1 q \right] dA - \int_{C^+ + C^-} t_i u_{i,1} q\, dC. \tag{B.19}$$

B.3. Application to thermal stress problems.

The application of the general result (B.11) to a particular class of problem merely requires that the tensor $\boldsymbol{H}$ contains the appropriate energy contributions, as defined by the crack tip energy integral (B.3), and that an explicit form of $\boldsymbol{h}$, the divergence of $\boldsymbol{H}^T$, be evaluated for the problem at hand. We consider here the uncoupled thermomechanical response of a deformation theory solid as outlined in Section 2 with the strain energy density as given by (2.7). Recalling that in this discussion $\boldsymbol{H}$ is given by

$$\boldsymbol{H} = W\boldsymbol{I} - \nabla\boldsymbol{u}\cdot\boldsymbol{\sigma} \tag{B.20}$$

we obtain

$$\boldsymbol{h} = \nabla\cdot\boldsymbol{H}^T = -\alpha\,\mathrm{tr}(\sigma)\,\nabla\theta + \boldsymbol{f}\cdot(\nabla\boldsymbol{u})^T. \tag{B.21}$$

This result is used in the expressions (B.9), (B.13) and (B.17) to yield particular forms of the domain integrals for the thermal stress problem (see (2.17), (2.10) and (2.20) in the text).

References

[1] J.W. Hutchinson, *Journal of Applied Mechanics* 50 (1983) 1042–1051.
[2] J.R. Rice, R.M. McMeeking, D.M. Parks and E.P. Sorensen, *Computer Methods in Applied Mechanics and Engineering* 17/18 (1979) 411–442.
[3] D.M. Parks, *International Journal of Fracture* 10 (1974) RCR 487–502.
[4] D.M. Parks, *Computer Methods in Applied Mechanics and Engineering* 12 (1977) 353–364.
[5] T.K. Hellen, *International Journal of Numerical Methods in Engineering* 9 (1975) 187–207.
[6] H.G. deLorenzi, *International Journal of Fracture* 19 (1982) 183–193.
[7] F.Z. Li, C.F. Shih and A. Needleman, *Engineering Fracture Mechanics* 21 (1985) 405–421.
[8] C. Atkinson and J.D. Eshelby, *International Journal of Fracture Mechanics* 4 (1968) 3–8.
[9] B.V. Kostrov and L.V. Nikitin, *Archiwum Mechaniki Stosowanej* 22 (1970) 749–775.
[10] L.B. Freund, *Journal of Elasticity* 2 (1972) 341–349.
[11] T. Nakamura, C.F. Shih and L.B. Freund, *International Journal of Fracture* 27 (1985) 229–243.
[12] Q.S. Nguyen, in *Three-Dimensional Constitutive Relations and Ductile Fracture*, edited by S. Nemat-Nasser, North-Holland Publishing Co., Amsterdam (1981) 315–330.
[13] J.R. Rice, in *Fracture: An Advanced Treatise*, edited by H. Liebowitz, Vol. 2, Academic Press (1968) 191–311.
[14] J.D. Eshelby, in *Inelastic Behavior of Solids*, edited by M.F. Kanninen et al., McGraw-Hill, New York (1970) 77–114.
[15] B. Budiansky and J.R. Rice, *Journal of Applied Mechanics* 40 (1973) 201–203.
[16] W.K. Wilson and I.-W. Yu, *International Journal of Fracture* 15 (1979) 377–387.
[17] S. Aoki, K. Kishimoto and M. Sakata, *Engineering Fracture Mechanics* 16 (1982) 405–413.
[18] H.G. deLorenzi, "Energy Release Rate Calculations by the Finite Element Method," General Electric Company TIS Report 82 CRD205 (1982).
[19] R.S. Barsoum, *International Journal for Numerical Methods in Engineering* 11 (1977) 85–98.
[20] M.A. Hussain, C.F. Shih, and M.D. German, "Lagrangian Elements as Singularity Elements in Crack Analysis," General Electric Company, Technical Information Series Report No. 80CRD291 (December 1980).
[21] D.S. Malkus and T.J.R. Hughes, *Computer Methods in Applied Mechanics and Engineering* 15 (1978) 63–81.
[22] C.F. Shih and A. Needleman, *Journal of Applied Mechanics* 51 (1984) 48–56.
[23] O.C. Zienkiewicz, *The Finite Element Method*, McGraw-Hill, London, England (1977).
[24] C.F. Shih, H.G. deLorenzi and W.R. Andrews, in *Elastic-Plastic Fracture*, ASTM STP 668, edited by J.D. Landes et al., American Society for Testing and Materials (1979) 65–120.
[25] B.R. Bass, R.H. Bryan, J.W. Bryson and J.G. Merkle, *Journal of Pressure Vessel Technology* 104 (1982) 308–316.
[26] B.R. Bass and J.W. Bryson, *International Journal of Fracture* 22 (1983) R3–R7.
[27] H.G. deLorenzi and C.F. Shih, *International Journal of Fracture* 21 (1983) 195–220.

RÉSUMÉ

En sa basant sur une intégrale simple exprimant le taux de relaxation d'énergie afférant aux champs de contrainte à l'extrémité d'une fissure, expression applicable à la réponse d'un matériau quelconque, on a déduit une intégrale de domaine (superficielle ou volumique) décrivant l'énergie dans un corps soumis à contraintes thermiques.

On fournit l'intégrale générale relative à un domaine fini tridimensionnel et à des cas particuliers bidimensionnels et axisymétriques, exprimant le taux de relaxation d'énergie. L'intégrale de domaine est naturellement compatible avec une formulation par éléments finis des équations de champ. Comme telle, elle convient idéalement pour un calcul facile et précis des valeurs ponctuelles du taux de relaxation de l'énergie le long du front d'une fissure tridimensionnelle. L'implantation d'éléments finis dans l'intégrale de domaine correspond à une technique d'extension virtuelle de la fissure. On discute des procédures de calculs du taux de relaxation de l'énergie, qui utilisent les solutions relatives au champ déterminées par voie numérique. A titre d'illustration, on présente plusieurs exemples numériques.